BLANKET DESIGN STUDIES OF A LEAD-BISMUTH EUTECTIC–COOLED ACCELERATOR TRANSMUTATION OF WASTE SYSTEM

ACCELERATORS

KEYWORDS: *accelerator-driven system, waste transmutation, lead-bismuth eutectic*

WON SIK YANG* and HUSSEIN S. KHALIL†
Argonne National Laboratory, 9700 South Cass Avenue, Argonne, Illinois 60439

Received September 25, 2000
Accepted for Publication February 8, 2001

The results of blanket design studies for a lead-bismuth eutectic (LBE)–cooled accelerator transmutation of waste system are presented. These studies focused primarily on achieving two important and somewhat contradictory performance objectives: First, maximizing discharge burnup, so as to minimize the number of successive recycle stages and associated recycle losses, and second, minimizing burnup reactivity loss over an operating cycle, to minimize reduction of source multiplication with burnup. The blanket is assumed to be fueled with a nonuranium metallic dispersion fuel; pyrochemical techniques are used for recycle of residual transuranic (TRU) actinides in this fuel after irradiation. The key system objective of high-discharge burnup is shown to be achievable in a configuration with comparatively high power density and relatively low burnup reactivity loss. System design and operating characteristics that satisfy these goals while meeting key thermal-hydraulic and materials-related design constraints have been preliminarily developed. Results of the performance evaluations indicate that an average discharge burnup of ~27% is achieved with a ~3.5-yr fuel residence time. Reactivity loss over the half-year cycle is 5.3%Δk. The peak fast fluence value at discharge, the TRU fraction in the charged fuel, and the peak coolant velocity are well within the assumed design limits. Owing to its use of nonuranium fuel, this proposed LBE-cooled system can consume light water reactor-discharge TRUs at the maximum rate achievable per unit of fission energy produced (~1.0 g/MWd).

I. INTRODUCTION

International interest in developing separations and transmutation technologies for waste management has been increasing over the last several years. As part of the accelerator transmutation of waste (ATW) program in the United States, preliminary trade studies are currently being performed at Argonne National Laboratory (ANL) and Los Alamos National Laboratory to define and compare candidate ATW systems. In this paper, we present the results of physics optimization studies for a lead-bismuth eutectic (LBE)–cooled ATW blanket.

The studies have so far focused primarily on the blanket component of the overall system, because the choice of blanket technologies is among the most important technical decisions faced in the ATW program. Both the basic technology and the particular features of the blanket design strongly impact transmutation performance and requirements on other ATW subsystems (spallation target, accelerator, and chemical separations). The LBE concept developed here is one of several blanket technology options currently under consideration in the ATW program. The plan is to conduct screening evaluations leading to the selection of two or three of the candidate concepts for further development and later to select a single preferred technology from among those retained in the initial screening process.[1]

Extensive discussions of the merits of LBE coolant and of the issues associated with its use in ATW can be found in the reports of the ATW roadmap working groups.[2,3] An in-depth summary of the key neutronic, thermal-hydraulic, material compatibility, coolant chemistry, and coolant activation characteristics of LBE and other fast reactor coolants is provided in Ref. 4.

*Permanent address: Chosun University, Department of Nuclear Engineering, 375 Seosuk-dong, Dong-gu, Kwangju 501-759, Korea.
†E-mail: khalil@ra.anl.gov

The organization of this paper is as follows: Sec. II describes the scope and objectives of the system point design development and outlines the assumptions employed in the development. Parametric studies conducted to evaluate tradeoffs associated with adoption of various design parameters and operating strategies are presented in Sec. III. Design parameters and performance characteristics for the blanket point design selected on the basis of these parametric studies are provided in Sec. IV. Section V summarizes conclusions of the system point design development studies and addresses requirements for (a) further development of the system point design, including subsystems other than the transmutation blanket, and (b) assessment of key "interface" issues affecting the coupling of the various subsystems.

II. SCOPE AND OBJECTIVES

The primary objective of the system development efforts at ANL has been to achieve efficient transmutation of the transuranic (TRU) actinides separated from light water reactor (LWR) spent fuel. It is generally recognized that a fast neutron energy spectrum is needed to accomplish the transmutation of minor actinides efficiently, because the fission-to-capture ratio for several key TRU nuclides is significantly greater in a fast spectrum.[5] The higher capture probability per incident neutron in a thermal spectrum causes buildup of the higher actinide fraction in the proportion of the TRU loading not consumed by fission, which adversely impacts neutron balance at high burnup and complicates recycle if the burnup is incomplete. On the other hand, the higher TRU inventory of fast systems for a given power level implies a lower specific power and a correspondingly lower burnup rate. Moreover, the fuel irradiation time in a fast spectrum is limited by radiation damage to structural materials caused by the large flux of high-energy neutrons. Consequently, fuel burnup in a fast system is generally incomplete in one pass through the transmutation blanket, and recycle of discharged fuel is required to achieve an acceptably low TRU content in the waste stream. It is assumed in the point design for the LBE system that fuel recycle is performed using pyrochemical techniques referred to as "PYRO-B" in the ATW roadmap.[6]

The major assumptions made in developing the LBE system point design are similar to those employed in the ATW roadmap as a basis for estimating ATW system costs and analyzing deployment scenarios; they can be summarized as follows:

1. A high-power linear accelerator generates a beam of energetic (~1 GeV) protons for delivery to a target/blanket "transmuter" system; the proton beam impinges on a spallation target and produces a source of neutrons that drives the subcritical blanket. The current system concept is to employ a single accelerator to drive four transmuters, and to deploy two accelerators (eight transmuters) at each ATW system site.

2. Beam delivery to the target is in the vertical direction; the target material is liquid LBE. The source neutrons are produced by direct impingement of the proton beam onto the LBE target in a process called spallation. A window cooled by the same LBE coolant provides the separation between the vacuum of the beam transport tube and the target.

3. The blanket is fueled with solid, uranium-free fuel clad with a low-swelling stainless steel alloy similar to the HT-9 alloy developed in the U.S. Advanced Liquid Metal Reactor (ALMR) Program.[7,8] The fission power level of each transmuter module is 840 MW(thermal)—consistent with the ALMR power level selected on the basis of favorable economics (through modular fabrication and installation) and excellent safety (passive removal of decay heat using ambient air as an inexhaustible heat sink).

4. The transmutation blanket is coupled to systems for heat removal, steam generation, and electricity production. The chemical inertness of LBE (no rapid reaction with air or steam/water) creates the possibility of eliminating the intermediate heat transport loop conventionally employed in sodium-cooled liquid-metal reactors (LMRs); steam generator modules can thus be placed in the vessel containing the transmuter and its primary heat removal system (pool-type arrangement).

5. Chemical separations required to extract uranium and fission products from the LWR discharge fuel is performed with the UREX process,[6] and the TRU-containing output stream from this process is treated with a subsequent pyrochemical process "PYRO-A" to produce metallic TRU feed for use in ATW fuel fabrication. Recovery of the TRUs remaining in the ATW fuel after irradiation in the ATW blanket is performed using the PYRO-B process.[6] To minimize off-site shipments of nuclear materials, the (modular) facilities required to accomplish the separations and to incorporate process wastes into durable waste forms suitable for disposal are collocated with the accelerator and transmutation subsystems at the ATW plant site.

6. Key long-lived fission products (LLFPs) (^{129}I and ^{99}Tc) are separately recovered during the LWR spent-fuel pretreatment steps. It has not yet been decided whether to immobilize these species in suitable waste forms or to transmute them in the ATW blanket. Accordingly, initial system development efforts have focused on transmutation of TRUs only. This approach provides a basis for future evaluations of overall system impacts of LLFP transmutation.

The central objective of the system development studies conducted to date has been to define the characteristics of a transmutation system that minimizes TRU losses to the waste streams. As shown in Sec. III, this objective is accomplished by maximizing the discharge burnup of ATW fuel (to minimize the number of recycle passes) and minimizing the fractional TRU loss per pass in recycle and refabrication. The achievable discharge burnup is believed to be constrained primarily by the fast-neutron irradiation damage to the cladding (fast fluence limit). The discharge burnup value currently targeted (~30 at.%) is high for conventional LMR fuels and remains to be demonstrated for the metallic dispersion fuel currently identified as the reference fuel form for the LBE-cooled transmuter. However, this burnup appears to be a reasonable development goal for the dispersion fuel type, particularly uranium-free fuels employing a nonfissioning matrix (e.g., zirconium or molybdenum); at a fixed heavy atom (fractional) burnup, the fission product density is much lower with a nonfissioning matrix than with a U matrix. Thus, to the extent achievable, fuel burnup is governed by fission product accumulation; higher burnup fractions can be targeted for nonuranium fuels.

Analyses of the LBE system point design have so far focused primarily on the equilibrium fuel cycle, because system performance under equilibrium conditions is believed to be a good basis for design optimization. Moreover, the analyses have mostly assumed a specific composition for LWR-discharge TRUs. Performance of the system under nonequilibrium conditions and for a range of LWR-discharge TRU compositions is of interest, but has been only preliminarily explored as discussed in Sec. III. In the equilibrium cycle, the charged fuel contains the TRUs recovered via recycle from the discharged fuel, supplemented by LWR-discharge TRUs to make up for the TRU deficit in the recycled component (i.e., for the ~30% TRU consumed by fission each cycle). Determination of the equilibrium composition has so far neglected the very small proportion of TRUs lost during recycle and refabrication.

III. PARAMETRIC STUDIES

This section describes parametric studies conducted to evaluate tradeoffs associated with adoption of various design parameters and operating strategies for the LBE transmutation system. These parametric studies have focused primarily on achieving two important and somewhat contradictory performance objectives: (a) maximizing discharge burnup, so as to minimize the number of successive recycle stages and associated recycle losses, and (b) minimizing burnup reactivity loss over an operating cycle, to minimize reduction of source multiplication with burnup.

A wide range of potential transmuter designs have been examined starting with the 840-MW(thermal) "pure burner" PRISM ALMR design previously developed at ANL for weapons-grade plutonium disposition.[5] The burner design was converted to an accelerator-driven LBE-cooled subcritical system by replacing the central assemblies with LBE target and buffer and the sodium coolant with LBE. To reduce the possible ranges of design parameters, a set of design constraints for an LBE-cooled system were first developed. Possible ranges of the coolant and fuel volume fractions and the blanket power density were derived based on these design constraints.

Within this reduced design parameter space, studies aimed at maximizing the discharge burnup were first pursued with the fuel residence time and cycle duration fixed. Variations in the fuel pin diameter and pitch (i.e., variations in fuel, coolant, and structure volume fractions), assembly height, and blanket size and arrangement were analyzed. Possible approaches to reducing the burnup reactivity loss while simultaneously achieving high-discharge burnup were subsequently investigated. In addition, the effects of variations of the fuel matrix material and of the LWR-discharge TRU composition were analyzed.

The remainder of this section is organized as follows: The rationale for the selected performance objectives is discussed in Sec. III.A. The imposed design constraints are presented in Sec. III.B, and computational methods applied in the various analyses are described in Sec. III.C. Parametric studies focused on discharge burnup maximization are summarized in Sec. III.D; these studies evaluate alternative assembly designs, blanket sizes and configurations, and fuel matrix materials, as well as the use of absorber materials. Finally, in Sec. III.E, blanket design approaches to reducing the burnup reactivity loss are described.

III.A. Performance Objectives

The main purpose of the ATW system is to facilitate spent-fuel disposal by removing the TRU elements and LLFPs from the spent fuel and transmuting these constituents in the ATW blanket. Accordingly, one practical measure for the performance of the ATW system is the fraction of the initial TRU inventory that is not transmuted and lost to the waste stream; minimization of this fraction is obviously desirable. As discussed later, the goal of minimizing this fractional loss motivates the design for maximum discharge burnup. On the other hand, the source multiplication in the subcritical blanket decreases with burnup due to the reactivity loss. To minimize the resulting needs for increasing accelerator power and/or introducing an excess reactivity that would have to be compensated via active reactivity control, it is desirable to minimize the burnup reactivity loss. Therefore, maximizing discharge burnup and minimizing

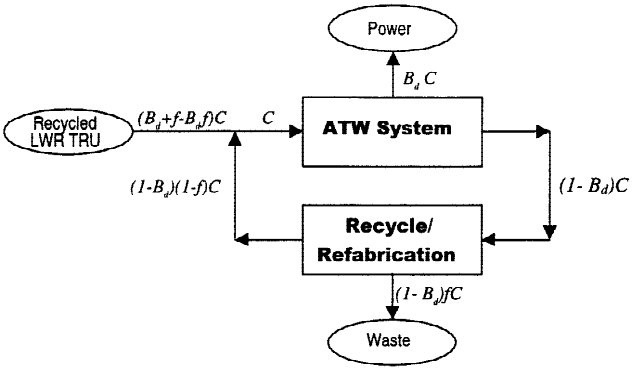

Fig. 1. Schematic diagram of TRU mass flows in the equilibrium cycle.

burnup reactivity loss over an operating cycle were chosen as the primary performance objectives in the physics design of the LBE-cooled blanket.

As illustrated in Fig. 1, if C is the equilibrium amount of TRUs charged to the blanket per cycle and B_d is the equilibrium-cycle fractional discharge burnup, then $B_d C$ is converted into energy and $(1-B_d)C$ is discharged from the blanket each cycle. Denoting the fraction of TRUs lost in recycle/refabrication as f, then $(1-B_d)(1-f)C$ is reloaded into the blanket, and the amount of LWR-discharge TRUs supplied as makeup for TRUs consumed by fission becomes $(B_d + f - B_d f)C$. Consequently, the fractional loss of the initial TRU inventory is given by

$$l_w = \frac{(1-B_d)f}{B_d + f - B_d f} \quad . \tag{1}$$

To minimize this fractional loss, it is necessary to maximize the fractional discharge burnup and minimize the fractional loss in recycle/refabrication. Achievement of high discharge burnup is thus an important goal for the ATW blanket design and fuel-development tasks.

The incentive to minimize burnup reactivity loss can be illustrated by noting that the fission power produced by the subcritical blanket varies with static reactivity ρ as

$$P_{fission} \propto SI_s/(-\rho) \quad , \tag{2}$$

where ρ is related to the effective multiplication factor $k(k < 1)$ as $\rho = 1 - 1/k$, S is the spallation neutron source, and I_s is the source importance factor.[9] As TRU actinides are depleted over an irradiation cycle, k decreases and ρ becomes more negative. Thus, without compensating measures, the fission power declines with fuel depletion (a) making it difficult to design an economic heat removal system and (b) if the system produces electricity, reducing the generation of electric power whose sale is intended to reduce net system cost.

The decline in blanket fission power over an irradiation cycle can be mitigated in three ways:

1. gradual addition of reactivity, e.g., by continuous replacement of depleted fuel with fresh fuel or by withdrawal of control rods; use of burnable poisons is not effective in the fast-neutron systems currently preferred for waste transmutation because of their ability to consume minor actinides efficiently.
2. increase of the neutron source strength S by gradually increasing beam power.
3. increase of the source importance factor, e.g., by reducing the fraction of source neutrons lost by leakage or through capture in the target.

Irrespective of the method used to compensate for the reactivity decline, there are strong economic and safety incentives to minimize the decline itself. For example, the use of control rods to compensate burnup reactivity loss adds to system complexity/cost and creates a potential accident initiator (inadvertent reactivity insertion through control rod withdrawal or ejection). Control on the accelerator beam current requires an accelerator that is "overdesigned" for the lower TRU depletion state early in the irradiation cycle and creates a potential for source increase accidents. Control on source importance would likely be similar in terms of cost/complexity as control rods and also introduces the possibility of accidental increases in source importance.

Burnup reactivity loss over an operating cycle $\delta\rho_c$ can be expressed as the product of an average reactivity loss rate and the irradiation time per cycle T_{ci} (T_{ci} is the product of the capacity factor and the cycle duration T_c). Analogously, discharge burnup B_d can be expressed as the product of the specific power P_s and the total fuel irradiation time nT_{ci}, where n is the number of irradiation cycles. Recognizing that the reactivity loss over a cycle $\delta\rho_c$ is roughly proportional to the cycle burnup B_c, i.e.,

$$\delta\rho_c \propto B_c = B_d/n = P_s T_{ci} \quad , \tag{3}$$

it is readily apparent that attainment of a high discharge burnup B_d and low burnup reactivity loss $\delta\rho_c$ requires a sufficiently large number of irradiation cycles n to limit the cycle burnup B_c.

III.B. Design Constraints

Denoting the average power density (in watts per cubic centimetre) as q_v, the total fuel residence time (in days) in the blanket as T_R, and the fuel volume fraction as v_f, the discharge burnup B_d (in at.%) can be represented as

$$B_d = cT_R q_v/v_f e_{\text{TRU}} \quad , \tag{4}$$

where e_{TRU} is the TRU mass per unit of fuel volume and c is a constant. This relation suggests that the discharge burnup can be maximized by designing for the maximum power density and fuel residence time and the minimum fuel volume fraction and TRU mass loading in the fuel. However, these quantities are interrelated and limited by various design constraints as described below.

With lead-based coolant, corrosion and erosive wear of core structural materials are intensified as coolant velocity increases, and hence, the coolant velocity must be limited.[10] Consequently, the coolant volume fraction must be large enough to provide adequate cooling. If the limiting coolant velocity (in metres per second) is V_c and the coolant temperature rise (in kelvin) is ΔT_c, the coolant volume fraction v_c should satisfy the following inequality:

$$v_c \geq \frac{p_f L_c q_v}{c_p \rho_c \Delta T_c V_c} \quad , \tag{5}$$

where

p_f = power-peaking factor

L_c = active core height (m)

ρ_c = coolant density (kg/m^3)

c_p = coolant specific heat (J/kg·K).

The peak linear power is constrained by the need to limit the peak fuel centerline temperature. To satisfy the peak linear power limit, the fuel volume fraction should satisfy the following inequality:

$$v_f \geq \frac{\pi}{4} \frac{s_p p_f d^2 q_v}{q'_m} \quad , \tag{6}$$

where

q'_m = limiting value of peak linear power (W/m)

d = fuel pin diameter

s_p = exposure-stage factor accounting for the higher power density of fresh fuel assemblies.

For the reference TRU-Zr metallic dispersion fuel[11] and LBE coolant, a peak linear power limit of 33 kW/m (derived on the basis of simple heat transfer calculations) is assumed, pending more detailed analytical and experimental evaluations.

The peak fast fluence and the discharge burnup are limited by the need to ensure the fuel pin integrity. In the proposed dispersion fuel where TRU-10Zr fuel particles are dispersed in a zirconium metal matrix, fission products are retained within the fuel particles, which are contained within the matrix. As a result, a higher burnup can be achieved compared to the conventional metallic fuel, and thus, the discharge burnup is not likely to constrain the design. On the other hand, there is likely a fast fluence limit for the core structural material (assumed to be a low-swelling stainless steel alloy similar to HT-9), and the peak fast fluence limit was assumed to be $\sim 4.0 \times 10^{23}$ n/cm^2. This peak fluence limit on the blanket structural material constrains the fuel residence time.

The TRU mass per unit of fuel volume (e_{TRU}) is determined such that the desired subcriticality level at the beginning of cycle (BOC) is achieved for the selected blanket configuration and fuel management scheme. This quantity is constrained by the maximum volumetric fraction of fuel particles (assumed here to be TRU-10wt%Zr) in the dispersion fuel. This maximum volume fraction is 50%, but lower volume fractions are preferred. A TRU-10Zr fuel particle volume fraction of 50% is equivalent to a TRU weight fraction of ~61% in the composite fuel.

The limitation on maximum coolant velocity constrains the allowable values of volumetric power density and coolant fraction. For a specified maximum coolant velocity, the minimum coolant volume fraction required for adequate cooling increases as the power density increases. On the other hand, the minimum fuel volume fraction required to satisfy the specified constraint on peak linear power increases as the power density increases, and hence, by volume conservation, the maximum coolant volume fraction decreases. Figure 2 shows the maximum and minimum coolant fractions estimated as functions of average power density for a peak linear power of 33 kW/m and typical values of core height (1.0 m), coolant temperature rise (150°C), and power-peaking factor (1.5). Consequently, as Fig. 2 shows, there exists an upper limit on the achievable power density. For example, if the coolant velocity limit is 2.0 m/s, then ~175 kW/ℓ is the maximum feasible power density for fuel pins of 0.635-cm diameter.

III.C. Computational Methods and Modeling Assumptions

Analyses of the LBE system point design have so far focused primarily on the equilibrium fuel cycle, because system performance under equilibrium conditions is believed to be a good basis for design optimization. Equilibrium cycle performance characteristics were calculated using the REBUS-3 fuel cycle analysis code.[12,13] In the REBUS-3 equilibrium cycle model, the charged fuel contains the TRUs recovered via recycle from the discharged ATW fuel, supplemented by LWR-discharge TRUs to make up for the TRUs consumed by fission. Determination of the equilibrium composition neglected the very small proportion of TRUs lost during recycle and refabrication and assumed 5% of the rare-earth fission products are carried over by the recycled ATW TRUs.

The TRU mass loading in the fuel that meets the targeted subcriticality level at beginning-of-equilibrium cycle (BOEC) ($k_{eff} = 0.97$) was determined using the REBUS-3 enrichment search techniques.[12] REBUS-3 also computes both batch-dependent and batch-averaged compositions at BOEC and end-of-equilibrium cycle (EOEC) for each specified depletion region. In this study, five

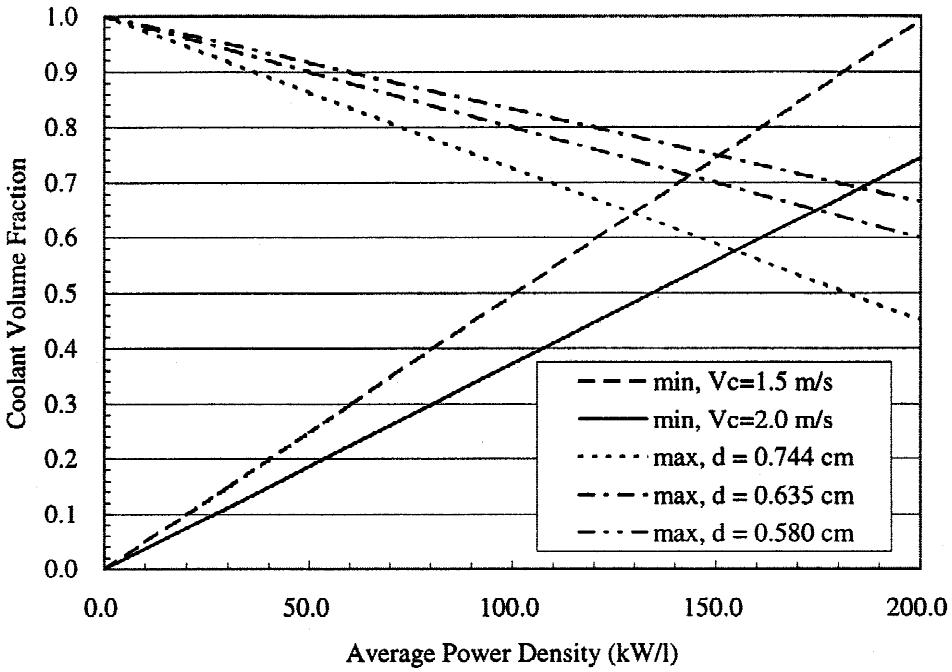

Fig. 2. Coolant volume fraction versus average power density.

(equal length) axial depletion zones were consistently used; in the planar direction, depletion zones consisted of individual fuel assemblies or of neighboring assemblies with similar reaction rates. Irradiation swelling of the fuel was modeled in the depletion calculations as a uniform 5% axial expansion of the fresh fuel, based on integral fast reactor experiments for U-Pu-Zr ternary metal fuel; this likely overestimates the expansion effect for the proposed dispersion fuel.

REBUS-3 flux calculations can be performed using a variety of neutronics solution options. To determine the sensitivity of the results to the choice of solution option, analyses for an 840-MW(thermal) ATW blanket design were performed using different flux computational options, solution geometries, and mesh sizes. An operating cycle length of 145 days (at an assumed capacity factor of 75%) and a six-batch refueling strategy were assumed. A scattered reloading scheme without fuel shuffling was employed, and two enrichment (TRU faction in charged fuel) zones were used to flatten the power distribution. A comparison was performed of solutions obtained using the nodal diffusion option in hexagonal-*z* geometry,[14] the finite difference options in triangular-*z* and *r*-*z* geometries,[15] and the VARIANT P_1 approximation in hexagonal-*z* geometry[16]; both the inhomogeneous source calculation and the corresponding homogeneous eigenvalue calculation (i.e., a system without the spallation source made artificially critical by use of an eigenvalue to scale neutron production) were considered in the comparison to determine whether the latter type of calculation can be employed in the parametric physics design studies. Region-dependent multigroup cross sections used in the neutronics analyses are based on ENDF/B-V.2 basic data and were generated for a 21-group energy structure using the MC^2-2 (Ref. 17) and SDX (Ref. 18) processing codes.

Table I compares the global equilibrium–cycle performance parameters for the various flux solution methods. These results show that the global performance parameters computed with different flux calculation methods are essentially the same. They also show that the integral parameters estimated with eigenvalue calculations are very similar to those obtained from inhomogeneous source calculations. Only the EOEC source multiplication factors differ significantly from the corresponding eigenvalues; this is attributed to differences in the flux distribution around the source region, which increase at EOEC due to the increased source intensity required to preserve the power level. These differences in the EOEC multiplication factor cause the indicated differences in burnup reactivity loss, because the burnup reactivity loss was simply estimated as the difference between the BOEC and EOEC multiplication factors.

Thus, for computational convenience, homogeneous (eigenvalue) neutronic calculations performed using the hexagonal-*z* nodal diffusion option of DIF3D were mostly employed as a basis for optimizing the global design parameters of the ATW blanket. For the detailed analyses of the proposed LBE system point design, however, inhomogeneous source problems were solved using a "generic" spallation neuron source distribution generated for a 1-GeV proton beam and a prototypic LBE

TABLE I

Comparison of Equilibrium Cycle Performance Parameters Obtained with Various REBUS-3 Flux Computation Options

Parameter	DIF3D-Nodal (Hexagonal-*z*)	VARIANT (Hexagonal-*z*)[a]	DIF3D-FD (6 tri/hex)[b]	DIF3D-FD (24 tri/hex)[c]	DIF3D-FD (*r*-*z*)
Homogeneous Eigenvalue Problem					
TRU fraction of fresh fuel (vol%)					
Low	22.26	22.31	22.22	22.28	22.18
High	26.71	26.77	26.66	26.74	26.62
Multiplication factor (eigenvalue)					
BOEC	0.97051	0.97001	0.96982	0.97012	0.96971
EOEC	0.91629	0.91583	0.91552	0.91590	0.91530
Burnup reactivity loss (%)	5.4	5.4	5.4	5.4	5.4
Average discharge burnup (MWd/kg)	262	261	262	262	263
TRU destruction rate (kg/yr)	237	237	237	237	237
BOEC TRU inventory (kg)	2361	2367	2356	2363	2351
Inhomogeneous Source Problem					
TRU fraction of fresh fuel (vol%)					
Low	22.36	22.43	22.35	22.42	22.34
High	26.83	26.92	26.82	26.90	26.81
Source multiplication factor					
BOEC	0.96958	0.96954	0.96970	0.97035	0.97044
EOEC	0.90932	0.90945	0.90957	0.91064	0.91022
Burnup reactivity loss (%)	6.0	6.0	6.0	6.0	6.0
Average discharge burnup (MWd/kg)	261	260	261	260	261
TRU destruction rate (kg/yr)	237	237	237	237	237
BOEC TRU inventory (kg)	2373	2380	2371	2379	2370

[a]P_1 approximation, 6th order polynomial inside a node, linear approximation for surface flux.
[b]Triangular-*z* geometry, 6 triangular meshes per hexagon.
[c]Triangular-*z* geometry, 24 triangular meshes per hexagon.

target.[19] Even though the spallation neutron source distributions depend on specific transmuter (target/blanket) configurations, the use of a generic source distribution appropriate to the accelerator beam proton energy and the spallation target material and geometry yields sufficiently accurate performance estimates. Moreover, for these system point design analyses, the flux calculation method was switched from the hexagonal-*z* nodal option to the triangular-*z* finite difference option of DIF3D to enable more accurate estimation of the peak flux, fluence, and burnup values.

III.D. Discharge Burnup Maximization Studies

In this section, optimization studies aimed at maximizing discharge burnup are presented. These studies were first focused on finding optimum values of such key system variables as power density (i.e., blanket size), fuel volume fraction, fuel residence time, etc., subject to the design constraints discussed in Sec. III.B. The analyses assumed a TRU-Zr dispersion fuel and a specific composition for LWR-discharge TRUs. After defining a partially optimized design on the basis of these studies, variations of the fuel matrix material and the LWR-discharge TRU composition were investigated.

As mentioned in Sec. III, the 840-MW(thermal) PRISM ALMR design was used as the starting point for the optimization studies. The burner design was converted to an accelerator-driven LBE-cooled subcritical system by replacing the central seven assemblies with LBE target and buffer and substituting LBE for the sodium coolant (see Fig. 3). The Pu-Zr binary metal fuel was changed to a TRU-Zr dispersion fuel, but the core structural material (HT-9) was retained, as were the compositions of the radial reflector and shield assemblies. For the parametric studies described in this section, fuel pin and assembly design parameters were varied while retaining the PRISM assembly lattice pitch [16 cm

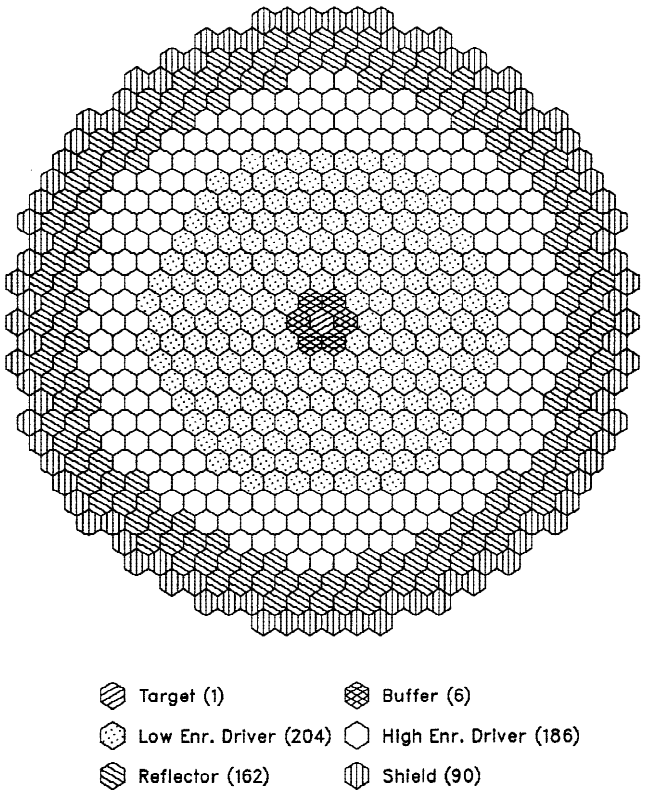

Fig. 3. ATW blanket configuration based on PRISM pure burner design.

(6.355 in.)]. The number of fuel assemblies and the active fuel height were also varied.

For the neutronics calculation model, the assembly design geometric data was modified by correction factors to account for axial fuel expansion and cold-to-hot dimensional changes. The active fuel height was increased by 5% in the neutronics model, and the fuel density was uniformly decreased by 5%. In addition, the fuel and structural materials were assumed to thermally expand when they were heated to operating temperatures. Uniform radial and axial expansion factors of 1.00596 and 1.00489 were assumed based on Type 316 stainless steel gridplate expansion and an HT-9 cladding expansion from room temperature to full-power conditions; thus, the fuel and structural densities were modified by a factor of 0.98338.

III.D.1. Effects of Blanket Size and Material Volume Fractions

Equation (4) suggests that the discharge burnup increases as the power density and the fuel residence time increase and as the fuel volume fraction and the TRU content of the fuel decrease. The TRU content of the fuel is determined by the requirement that the multiplication factor at BOEC satisfies a desired value, e.g., 0.97. Thus, it is a function of blanket size, material volume fractions, cycle duration, number of batches, etc. Consequently, the discharge burnup also depends on these factors in addition to being proportional to the power density and fuel residence time. To meet the high discharge-burnup goal, optimum values of blanket size and material volume fractions were first investigated with the fuel residence time and cycle duration fixed.

The LBE-cooled subcritical system obtained by minimally modifying the PRISM pure burner design has an average power density of 80 kW/ℓ. However, in order to increase the burnup rate, it is desirable to increase the power density as close to the maximum feasible value as possible. Furthermore, a more compact blanket configuration through a higher power density is desirable to decrease the system cost. Thus, several 840-MW(thermal) blanket configurations with higher power density were developed by reducing the number of assemblies. The average power density was varied up to 165 kW/ℓ, which is about the maximum power density achievable with the fuel pin diameters considered. The smaller number of fueled assemblies reduces the heavy metal inventory requirements and thus increases the rate of TRU consumption as a fraction of the initial inventory (increases burnup rate). Moreover, fuel cycle costs are reduced because fewer fuel pins and assemblies would have to be fabricated.

Equation (5) indicates that the maximum power density increases as the pin diameter decreases. Accordingly, in developing the higher power-density ATW configurations, the fuel pin diameter was reduced from the PRISM value (0.744 cm) to that of the Fast Flux Test Facility (0.580 cm) while retaining the PRISM hexagonal assembly lattice pitch. The number of fuel pins per assembly was correspondingly varied between 96 and 271 to obtain adequate coolant volume fractions.

Figure 4 shows the required TRU weight fraction in fuel (assuming the TRU density is 15.9 g/cm^3 and the Zr density is 6.5 g/cm^3) for a fixed fuel residence time as a function of the fuel volume fraction and the effective blanket diameter (excluding the reflector and shield). A fuel residence time of 3 yr at 75% capacity factor was assumed with a cycle length of 1 yr. The TRU weight fraction in fuel was calculated in each case such that the multiplication factor at BOC is 0.97. These results show that the required TRU content in the fuel decreases monotonically as the fuel volume fraction or the blanket size increases. The small fluctuations around the smooth fitting lines are due to the variations in cladding thickness and blanket geometry.

Since the TRU weight fraction in the fuel is a monotonic function of fuel volume fraction and blanket size, the discharge burnup is also a monotonic function of these variables in the variable domain of interest. Figure 5 shows the discharge burnup calculated (for fixed fuel residence time) as a function of fuel volume fraction and equivalent blanket diameter; the curves in Fig. 5 are

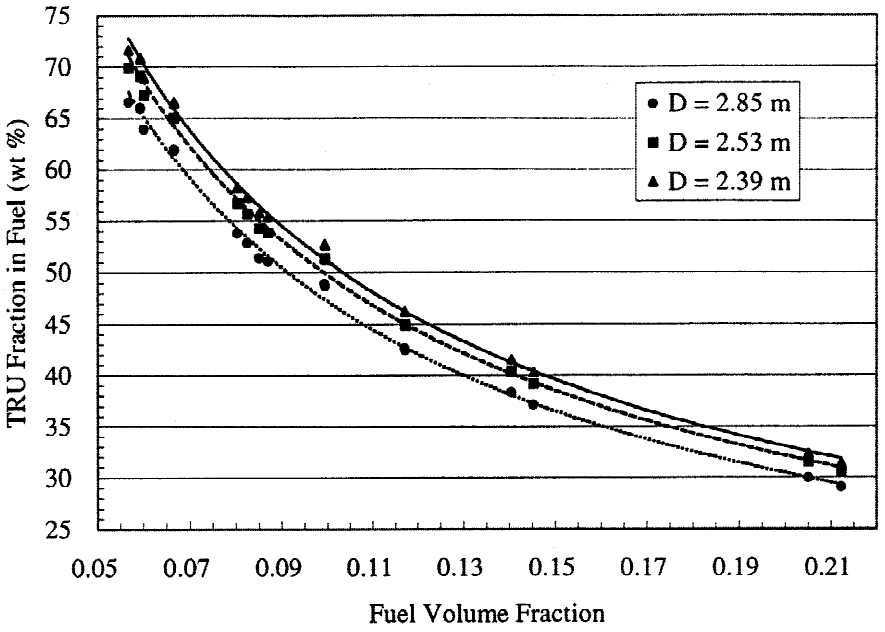

Fig. 4. TRU fraction of charged fuel versus fuel volume fraction and effective fuel region diameter (D).

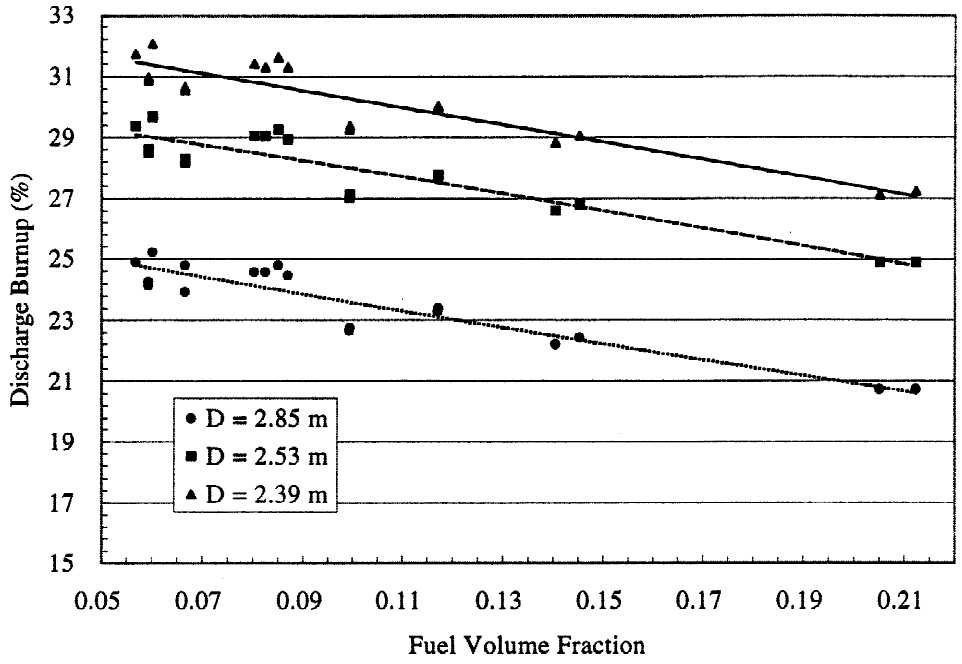

Fig. 5. Discharge burnup versus fuel volume fraction and effective fuel region diameter (D).

least-squares fits. As shown in Fig. 5, the discharge burnup increases monotonically as the fuel volume fraction or the blanket size decreases. These results indicate that there is no extreme point in the variable domain of interest, and hence, the maximum discharge burnup is obtained by designing for the minimum fuel volume fraction and blanket size. The minimum blanket size is constrained by the maximum coolant velocity and the peak linear power. The minimum fuel volume fraction is limited by the smallest feasible pin diameter and the highest TRU content feasible in the dispersion fuel form. In other words, for a fixed fuel residence time, the achievable

discharge burnup is limited by fuel fabrication and thermal-hydraulic design constraints.

Since the same amount of energy is produced for a fixed power level and fuel residence time, the maximum discharge burnup obviously corresponds to the minimum TRU inventory in the blanket. The preceding results show that the minimum inventory is achieved through minimum blanket size and pin diameter and maximum TRU content in the fuel. However, this minimum fuel inventory yields the largest burnup reactivity loss because the burnup reactivity loss is proportional, for fixed-cycle duration, to the discharge burnup as discussed in Sec. III.E.

The preceding results also indicate that the maximum discharge burnup achievable with 3-yr residence time is ~30% under reasonable fuel fabrication and thermal-hydraulic design constraints. The TRU fraction in fuel required to attain this burnup level is ~30% by volume, which corresponds to a 51% TRU mass fraction in the fuel. To increase the discharge burnup significantly over 30%, the fuel residence time would have to be increased. The allowable increase in fuel residence time is limited by the peak fluence limit on the structural material. The peak fast fluence based on a three-batch annual refueling scheme is compared for the zirconium and molybdenum matrix fuels as functions of burnup in Fig. 6. Figure 6 shows that the peak fast fluence is proportional to the discharge burnup for both the zirconium and the molybdenum matrix cases. It can be also seen from Fig. 6 that the maximum discharge burnup achievable with these dispersion fuels is ~29% under the peak fast fluence limit assumed for HT-9 cladding ($\sim 4.0 \times 10^{23}$ n/cm^2). These results indicate that the achievable discharge burnup would be constrained primarily by the fast-fluence irradiation damage to the cladding (fast fluence limit).

Based on the results of the foregoing parametric studies, a preliminary LBE-cooled blanket was developed to achieve the targeted high discharge burnup under the constraints discussed in Sec. III.B. Because the discharge burnup increases monotonically as the blanket size decreases, the relatively compact 192-fuel-assembly design shown in Fig. 7 was selected as the blanket geometry. To attain the discharge burnup of ~29% achievable under the peak fast fluence limit (see Fig. 6), the required fuel volume fraction appropriate for the selected blanket configuration was determined from Fig. 5 to be ~0.14. The corresponding TRU mass fraction in the fuel required for the three-batch annual refueling scheme was found to be ~42% (see Fig. 4). To attain the targeted fuel volume fraction of ~0.14 while satisfying the thermal-hydraulic constraints previously discussed, a fuel pin diameter of 0.635 cm was selected.

The principal design parameters of this preliminary design are summarized in Table II. For this design, equilibrium fuel cycle analyses were performed with a six-batch semi-annual refueling scheme as well as a three-batch annual refueling scheme to investigate the effects of cycle length on burnup reactivity loss. The total fuel residence time was kept the same in all cases, in keeping with the constraint on peak fast fluence. Neutronics calculations were performed using the hexagonal-*z* nodal

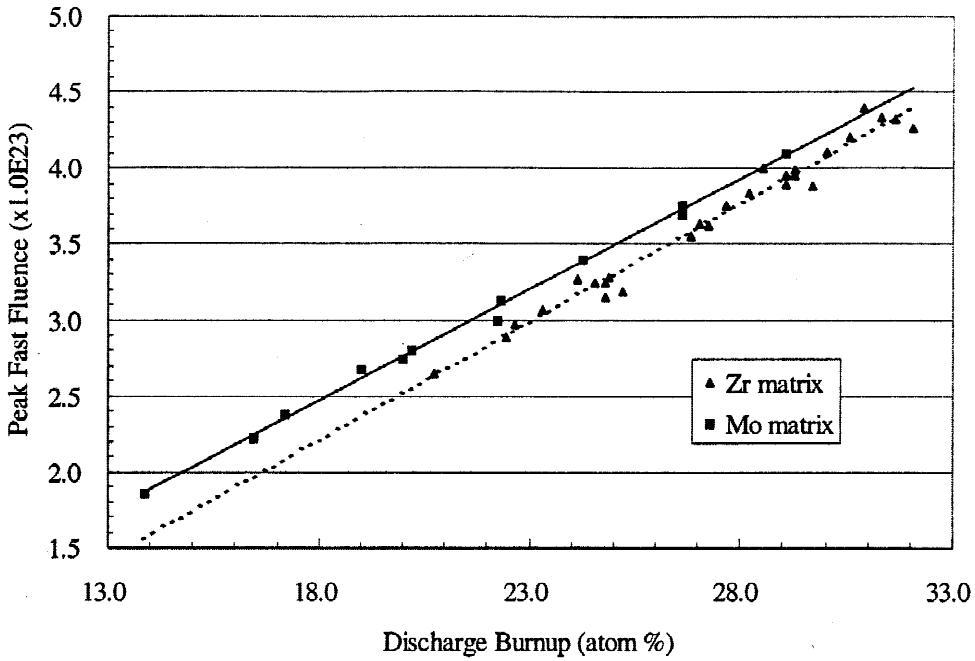

Fig. 6. Peak fast fluence versus discharge burnup.

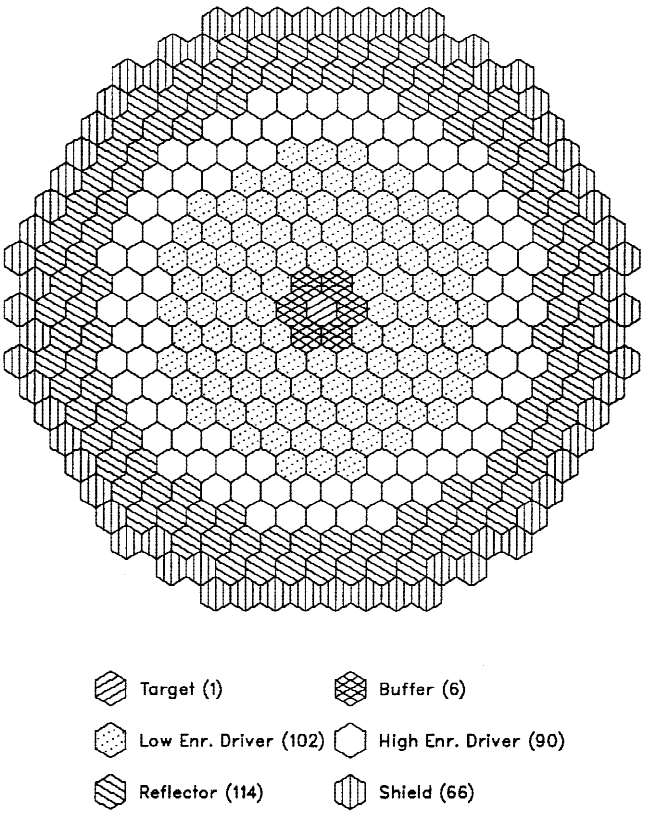

Fig. 7. Preliminary ATW blanket configuration (192 fuel assemblies).

TABLE II

Design Parameters for the Preliminary LBE-Cooled Blanket Design

Pin diameter (cm)	0.635
Cladding thickness (cm)	0.056
Pitch-to-diameter ratio	1.727
Number of pins per assembly	217
Fuel smear density (%)	75
Volume fraction (at operating temperature)	
Fuel	0.140
Structure	0.103
Coolant	0.695
Hexagonal assembly pitch (cm)	16.142
Number of assemblies	
LBE target/buffer	7
Fuel	
Inner zone	102
Outer zone	90
Total	192
Reflector	114
Shield	66
TRU fraction split factor (outer zone/inner zone)	1.2
Active fuel height (cm)	106.68
Equivalent fuel region diameter (cm)	239.11
Maximum blanket diameter (cm)	345.20

diffusion option of DIF3D, run in the eigenvalue mode. The TRU composition of a 10-yr–cooled PWR spent fuel of 33 MWd/kg burnup was used to represent the composition of the LWR-discharge TRU feed stream used as make up for the TRUs consumed by fission during each cycle.

Neutronics performance parameters are compared in Table III. These results show that a discharge burnup of ~29% is achievable with the assumed 3-yr fuel residence time. The TRU mass fractions of the fuel required to obtain the targeted BOEC k_{eff} of 0.97 are well below the limit for dispersion fuel, even though a higher TRU fraction is used in the outer blanket zone than the inner zone to flatten the power distribution. The highest outer-zone value (46.2 wt%) is equivalent to ~33 vol% of TRU-10Zr fuel particles in the dispersion fuel. Performance characteristics obtained for the three-batch annual and six-batch semiannual fuel management schemes

TABLE III

Performance Parameters for the Preliminary LBE-Cooled Blanket Design

	Annual Cycle	Semiannual Cycle
Number of fuel batches	3	6
Cycle irradiation time (days)	273	145
TRU fraction in fuel (wt%)		
Inner zone	38.6	40.3
Outer zone	44.3	46.2
Multiplication factor		
BOEC	0.9695	0.9702
EOEC	0.8566	0.9123
Burnup reactivity loss (% Δk)	11.3	5.8
Core-average power density (kW/ℓ)	166.0	166.0
Power-peaking factor		
BOEC	1.45	1.45
EOEC	1.45	1.45
Peak linear power (kW/m)	30.4	30.7
Discharge burnup (at.%)		
Average	29.1	29.1
Peak	39.9	39.9
Peak fast fluence (10^{23} n/cm^2)	3.91	3.96
Net TRU consumption rate (kg/yr)	237	237
Equilibrium loading (kg/yr)		
LWR TRU	237	237
Recycled TRU	581	579
Total TRU	818	816
Heavy metal inventory (kg)		
BOEC	2192	2256
EOEC	1955	2130

are generally very similar, except for the burnup reactivity loss. By adopting the six-batch semiannual refueling scheme instead of three-batch annual refueling, the burnup reactivity loss is halved without affecting discharge burnup. The semiannual cycle case requires a slightly higher TRU fraction in the charged fuel, because the smaller proportion of the blanket (one-sixth) refueled each cycle in this case yields a slightly higher average burnup at BOEC. This results in an increased BOEC TRU inventory.

III.D.2. Fuel Matrix Material Variations

As an alternative to the zirconium matrix of the reference metallic-dispersion fuel form, the use of molybdenum matrix was considered, primarily because of its greater compatibility with the LBE coolant, implying that a potential fuel pin failure might be more benign. Furthermore, molybdenum is a stronger absorber than zirconium; its use therefore increases the TRU inventory (which affects fractional TRU burnup and reactivity loss rates) and possibly introduces some Doppler feedback, which might be an important factor in mitigating the consequences of severe accidents.

To estimate the Doppler feedback contribution of the molybdenum matrix, a preliminary analysis was performed using the continuous-energy VIM Monte Carlo code.[20] The results showed that the molybdenum matrix provides no significant Doppler feedback. Additional parametric studies were performed to compare the fuel cycle performance of systems using molybdenum- and zirconium-based fuels. For fixed values of BOC multiplication factor (k_{eff} = 0.97), fuel residence time, and cycle length, the BOC TRU inventory was found to be ~33% greater with the molybdenum matrix than with zirconium, due to the significantly greater Mo absorption cross section. As a result, discharge burnup and burnup reactivity loss with the Mo matrix fuel were each reduced by ~23% compared to corresponding values with the Zr matrix.

The peak fast fluence and the burnup reactivity loss based on a three-batch annual refueling scheme were compared for the two matrix materials as functions of burnup. As previously shown in Fig. 6, the peak fast fluence is proportional to the discharge burnup for both the zirconium and the molybdenum matrix case. It can also be seen from Fig. 6 that the maximum discharge burnup achievable with the molybdenum matrix is slightly lower than that of the zirconium matrix fuel for a given peak-fast-fluence limit. In other words, under the same peak-fast-fluence limit, a slightly higher discharge burnup can be achieved with the zirconium matrix fuel than with the molybdenum. Figure 8 compares the burnup reactivity loss based on a three-batch annual refueling scheme for the two matrix materials as functions of burnup. It can be seen from Fig. 8 that the burnup reactivity loss becomes slightly higher with the molybdenum matrix fuel when based on the same discharge burnup. (To achieve the same discharge burnup, the molybdenum matrix fuel requires a higher power density or a longer

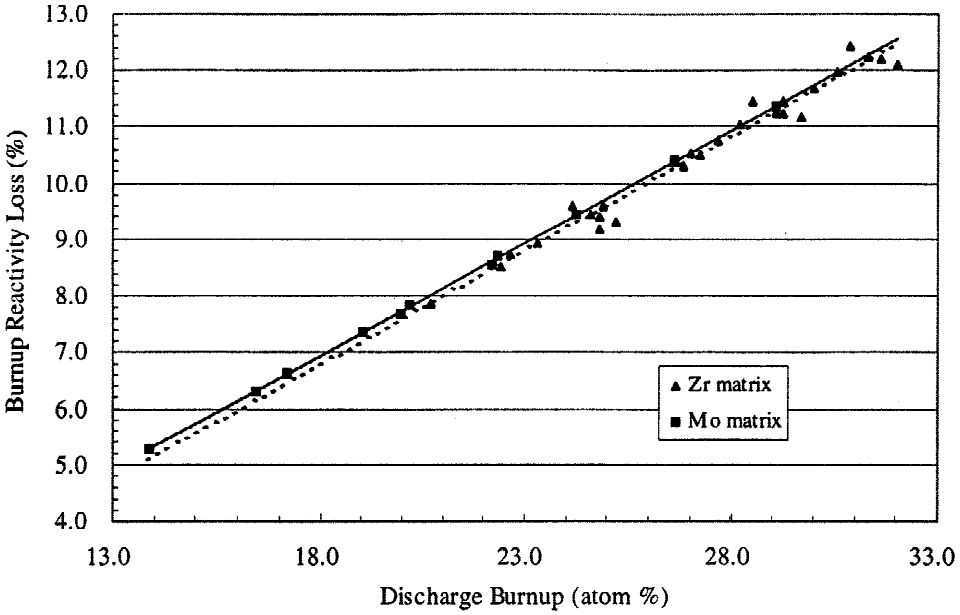

Fig. 8. Burnup reactivity loss versus discharge burnup.

residence time.) These results suggest that the molybdenum matrix has no advantage over the zirconium matrix from the neutronics point of view.

III.D.3. Effect of LWR Discharge Composition Variations

The isotopic composition of the LWR-discharge TRU used in the previously described parametric studies was derived from ORIGEN-2 (Ref. 21) depletion calculations for a typical PWR assembly with a nominal burnup of 33 MWd/kg and 10-yr cooling time. Because the LWR spent-fuel inventory to be transmuted by ATW systems would in reality be composed of spent-fuel assemblies differing in assembly type, burnup level, and cooling time, the ATW blanket needs to be designed with sufficient flexibility to accommodate different feed stream compositions; the option of blending different TRU feed streams to maintain a composition within a narrow range may not be feasible in practice. An investigation of the effects of different feed stream TRU compositions on neutronics and fuel cycle performance characteristics is described in this section.

For the preliminary LBE-cooled blanket configuration described in Sec. II.D.2, equilibrium fuel cycle analyses were performed using two different feed streams: 10- and 30-yr–cooled PWR spent fuel of 33 MWd/kg burnup. Table IV compares the isotopic compositions of these two feed streams, based on 99.995% uranium removal. The main difference between the two compositions is in the ^{241}Pu and ^{241}Am proportions, due to the relatively short half-life of ^{241}Pu (~14 yr); the other isotopic fractions are fairly similar. The effect of this composition difference on the computed equilibrium-cycle performance parameters is summarized in Table V for the three-batch annual refueling schemes. For fixed values of BOC multiplication factor (k_{eff} = 0.97), fuel residence time, and cycle length, the BOC TRU inventory is seen to be slightly greater (by ~3% for annual refueling and by ~2.5% for semiannual refueling) with the 30-yr–cooled feed stream composition than with 10-yr–cooled composition. This inventory difference is due to the lower fissile (^{241}Pu) and higher fertile (^{241}Am) fractions in the 30-yr–cooled feed stream. As a result of the higher inventory, discharge burnup and burnup reactivity loss are lower with the 30-yr–cooled feed stream. However, the differences are not large, suggesting that variations in LWR-discharge composition can be readily accommodated and that the use of a "standard" LWR spent-fuel composition as a basis for design optimization is appropriate.

TABLE IV

Isotopic Composition (wt%) of a PWR Assembly of 33 MWd/kg Burnup

	10-yr Cooling	30-yr Cooling
^{235}U	0.004	0.004
^{236}U	0.002	0.002
^{238}U	0.477	0.479
^{237}Np	4.839	5.101
^{238}Pu	1.428	1.225
^{239}Pu	53.101	53.227
^{240}Pu	21.437	21.550
^{241}Pu	7.770	2.976
^{242}Pu	4.675	4.689
^{241}Am	5.127	9.709
^{242m}Am	0.015	0.014
^{243}Am	0.925	0.926
^{243}Cm	0.003	0.002
^{244}Cm	0.184	0.086
^{245}Cm	0.009	0.009
^{246}Cm	0.001	0.001

TABLE V

Comparison of Blanket Performance Parameters for Two LWR TRU Feed Streams

	Spent Fuel Cooling Time	
	10 yr	30 yr
TRU fraction in fuel (wt%)		
Inner zone	38.6	39.4
Outer zone	44.3	45.1
Cycle irradiation time (days)	273	273
Multiplication factor		
BOEC	0.9695	0.9699
EOEC	0.8566	0.8654
Burnup reactivity loss (% Δk)	11.3	10.5
Power-peaking factor		
BOEC	1.45	1.45
EOEC	1.45	1.45
Peak linear power (kW/m)	30.4	30.1
Discharge burnup (at.%)		
Average	29.1	28.4
Peak	39.9	39.3
Peak fast fluence (10^{23} n/cm^2)	3.91	3.88
Net TRU consumption rate (kg/yr)	237	237
Equilibrium loading (kg/yr)		
LWR TRU	237	237
Recycled TRU	581	602
Total TRU	818	839
Heavy metal inventory (kg)		
BOEC	2192	2257
EOEC	1955	2020

III.E. Burnup Reactivity Loss Reduction Studies

The preliminary LBE-cooled blanket configuration described in Sec. III.D.1 was developed with the main objective of achieving high discharge burnup. In fact, this design yields the highest discharge burnup feasible under the peak-fast-fluence constraint, which appears to be the limiting parameter for discharge burnup. On the other hand, this preliminary configuration also yields the largest burnup reactivity loss for the selected (fixed) values of fuel residence time and cycle duration, because the burnup reactivity loss is (under these conditions) proportional to the discharge burnup as shown in Fig. 8. As discussed in Sec. III.B, reduction of the burnup reactivity loss while retaining high discharge burnup requires an increased number of irradiation cycles to limit the cycle burnup. Reduction of cycle burnup (to reduce reactivity loss over the cycle) can be accomplished by decreasing the specific power or the cycle length [see Eq. (3)].

These two possible approaches to reducing burnup reactivity loss while simultaneously achieving high discharge burnup were studied. The first approach is to reduce the cycle length while retaining the comparatively high specific power of the preliminary blanket design. Keeping the 3-yr fuel residence time (at 75% capacity factor), which is the longest irradiation time feasible under the peak-fast-fluence constraint assumed for the HT-9 structural material, the number of irradiation cycles was increased to six from three; this results in a half-year cycle duration. As shown in Table III, the (fluence-constrained) discharge burnup for this six-batch system is close to 30%. The burnup reactivity loss for this system is reduced from ~11 to ~5.8% by adopting a 6-month instead of 1-yr cycle duration. Further reduction of the burnup reactivity loss to ~3% should be feasible with a 3-month cycle—at the expense of an increase to 12 in the number of irradiation cycles and in the associated number of fuel management batches.

The alternative blanket design approach is to design for a low specific power and comparatively long cycle duration. Design requirements are apparent if the specific power is expressed as

$$P_s = c q_v / v_f \rho_{\mathrm{TRU}} \ , \qquad (7)$$

where

q_v = average power density

v_f = fuel volume fraction

ρ_{TRU} = TRU density in fuel

c = a constant.

This relation shows that the targeted low specific power can be achieved by designing for low power density and high TRU-loading density. To obtain a low power density, the large blanket configuration derived from the PRISM pure burner design (see Fig. 3) was used. To obtain a high TRU-loading density, an absorbing material (hafnium) was employed in the fuel assemblies. The use of hafnium (a resonance absorber) not only raises the fuel inventory needed to achieve a specified multiplication factor k, but also contributes a (small) negative Doppler effect. Design parameters of this system are compared in Table VI with those of the high specific-power system.

Equilibrium cycle analyses of the low specific power configuration were performed with an operating cycle length of 12 months at a capacity factor of 75%. The longest feasible total fuel irradiation time was found to be 10 yr under the assumed peak fast fluence constraint of 4.0×10^{23} n/cm^2. The TRU loading was calculated such that k at BOC is 0.97. Calculated performance characteristics for this system are compared in Table VII with those of the high specific-power system described earlier. The burnup reactivity loss of the low specific-power system (3.1%) is significantly lower than that of the high specific-power system (with either annual or semiannual refueling), but its discharge burnup is also somewhat lower despite a significantly longer fuel residence time (10 yr). Moreover, the blanket volume and TRU inventory are substantially larger than the corresponding quantities for the high specific-power system. Fundamentally, the low specific-power system exhibits a low reactivity loss because of the large number of fuel management batches; a comparably small cycle reactivity loss could be attained with the higher power density system by using the same number of batches (and proportionally reducing cycle duration).

The particular effect of employing the hafnium absorber was also examined by analyzing the performance of the low specific-power system with the hafnium removed from the fuel. As discussed in Sec. III.D.2 in

TABLE VI

Comparison of Design Parameters for the Low and High Specific-Power Designs

Parameter	Low Specific-Power Design	High Specific-Power Design
Fuel pin outer diameter (cm)	0.744	0.635
Cladding thickness (cm)	0.056	0.056
Pitch-to-diameter ratio	1.474	1.727
Hexagonal assembly pitch (cm)	16.14	16.14
Number of fuel assemblies	390	192
Volume fractions		
TRU-Zr fuel	0.115	0.140
HT-9 structure	0.150	0.103
Hf-Zr absorber	0.142	– – –
LBE coolant	0.593	0.695
Maximum blanket diameter (m)	4.44	3.45

TABLE VII

Comparison of Performance Characteristics for the Low and High Specific-Power Designs

	Low Specific-Power Design	High Specific-Power Design	
		Annual Cycle	6-Month Cycle
Number of fuel batches	10	3	6
Cycle length (days)	273	273	145
Burnup reactivity loss (% Δk)	3.1	11.3	5.8
Core-average power density (kW/ℓ)	83.0	166.0	166.0
Power-peaking factor	1.59	1.45	1.45
Peak linear power (kW/m)	14.0	30.4	30.7
Average discharge burnup (at.%)	25.8	29.1	29.1
Peak fast fluence (10^{23} n/cm^2)	3.95	3.91	3.96
Net TRU consumption rate (kg/yr)	242	237	237
Equilibrium loading (kg/yr)			
LWR TRU	242	237	237
Recycled TRU	700	581	578
Total	942	818	815
BOEC heavy metal inventory (kg)	8249	2192	2256

connection with use of molybdenum as a fuel matrix, an absorber increases the required TRU loading to achieve the desired subcriticality at BOC, and hence reduces the discharge burnup for a fixed residence time. Without the hafnium absorber, the equilibrium TRU loading is reduced by ~31%, the discharge burnup (for fixed irradiation time) is increased by ~42%, and the burnup reactivity loss is increased from 3.1 to 5.1%Δk.

In summary, the goal of achieving a low burnup reactivity loss, which is important for reasons of economics and safety, can be attained by design for either a low specific power or a short irradiation cycle time (or both). The low specific-power approach requires a low power density and high TRU inventory, as well as a large number of irradiation cycles (and fuel management batches) to achieve the targeted high discharge burnup. The short irradiation-cycle approach, which permits a blanket with higher power density and specific power, requires more frequent refueling. This latter approach is preferred at the present time because it employs a more compact (economical) blanket and because the more frequent refueling may not adversely impact system availability given the likely need for periodic shutdown for maintenance or replacement of accelerator, beam delivery, and spallation target components.

IV. SYSTEM POINT DESIGN SPECIFICATIONS AND PERFORMANCE

This section describes the development of an LBE-cooled blanket point design based on the results of parametric studies described in Sec. III.E. As a first step in specifying this point design, inhomogeneous source calculations were performed for the preliminary design described in Sec. III.E. Because the spallation neutron source is concentrated in the target, explicit modeling of the source via inhomogeneous flux calculations yields higher peak fluxes and a higher peak power density than the corresponding eigenvalue calculation. This peaking of the flux and power occurs in one of the innermost fuel assemblies (at a surface facing the target), and it increases over an irradiation cycle because the source intensity required to maintain the constant power level increases. As a result, the peak-fast-fluence value predicted by the inhomogeneous calculation is considerably higher than that of the eigenvalue solution.

To reduce the power-peaking factor and the peak-fast-fluence value, the preliminary design was further refined. First, the intensity of the inhomogeneous source at the interface between the LBE buffer and the innermost fuel assemblies was reduced by extending the buffer region surrounding the central target region from one to two rows of assemblies. Second, to reduce the peak linear power, the number of pins per assembly was increased to 271 from 217 while preserving the optimum fuel and coolant volume fractions by reducing the pin diameter from 0.635 to 0.580 cm. The cladding thickness was increased from 0.056 to 0.070 cm to provide an additional margin to pin failure through corrosive wear due to the LBE coolant. Third, the blanket power distribution was further flattened by optimizing the split of the TRU loading among concentric planar zones of the blanket. Three different blanket zones differing in the

TRU mass fraction of the fuel (i.e., in "enrichment") were employed, and the zone sizes and enrichments were determined such that the peak linear powers of the three zones are close to each other.

A semiannual cycle with 75% capacity factor was employed. A seven-batch fuel management scheme was adopted for the middle and outer blanket zones to maximize the fuel residence time and discharge burnup within the peak-fast-fluence constraints. The fuel residence time in the innermost zone was limited to six cycles to limit the peak fast fluence. To minimize fluctuations of system performance characteristics, cycle-to-cycle variations of the number of assemblies refueled in each blanket zone should be minimized. Accordingly, the blanket configuration was specified such that the number of assemblies in each blanket zone is an integer multiple of the corresponding number of fuel batches. The proposed blanket layout is shown in Fig. 9; it consists of 19 hexagonal lattice positions containing the LBE target/buffer and 204 fuel assemblies. The blanket is surrounded by two hexagonal rows of steel reflector assemblies and one row of B_4C shield assemblies. The principal design parameters of the proposed design are summarized in Table VIII.

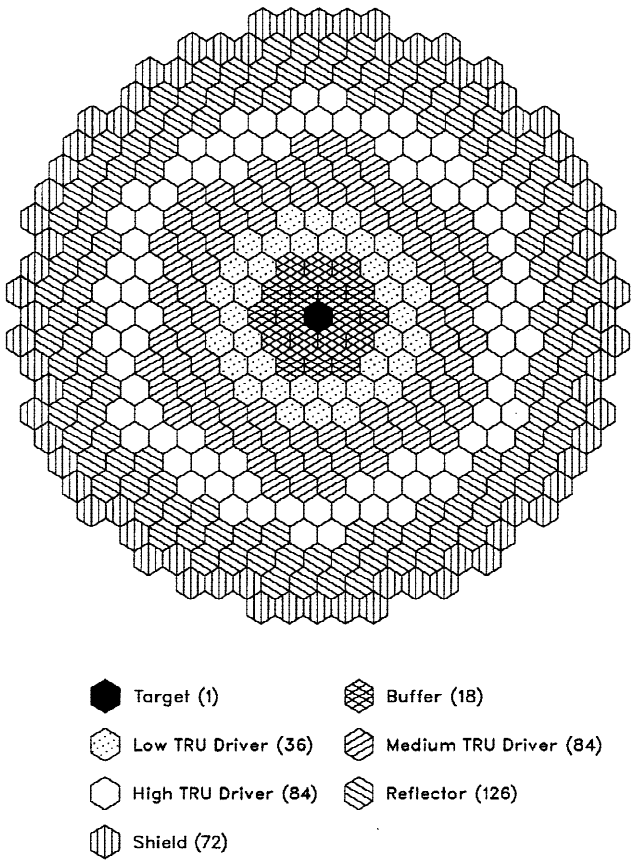

Fig. 9. Proposed LBE-cooled blanket configuration (204 fuel assemblies).

TABLE VIII

Design Parameters for the Proposed LBE-Cooled Blanket Point Design

Proton energy (GeV)	1.0
Target material	LBE
Fuel material	(TRU-10Zr)-Zr
Pin diameter (cm)	0.580
Cladding thickness (cm)	0.070
Pitch-to-diameter ratio	1.691
Number of pins per assembly	271
Fuel smear density (%)	85
Volume fraction (at operating temperature)	
Fuel	0.142
Structure	0.138
Coolant	0.682
Hexagonal assembly pitch (cm)	16.142
Number of assemblies	
LBE target/buffer	19
Fuel	
Inner zone	36
Middle zone	84
Outer zone	84
Total	204
Reflector	126
Shield	72
TRU fraction split factor (outer/ middle/ inner zone)	1.45/1.28/1.00
Active fuel height (cm)	106.68
Equivalent fuel region outer diameter (cm)	253.12
Maximum blanket diameter (cm)	359.98
Number of fuel batches	
Inner zone	6
Middle and outer zones	7
Cycle irradiation time (day)	137

The equilibrium-cycle neutronics performance of the proposed point design was analyzed using the REBUS-3 code. The (inhomogeneous) flux calculations were performed with the triangular-*z* finite difference option of DIF3D using a generic spallation neutron source distribution generated for a 1-GeV proton beam and a prototypic LBE target.[19] A medium burnup (33 000 MWd/tonne) PWR assembly with a 25-yr cooling time was used to specify a composition of the LWR-discharge feed stream.[22] The isotopic composition of this feed stream is compared in Table IX with the equilibrium-cycle ATW discharge composition. The fuel enrichments in each blanket zone were determined according to the enrichment split factors shown in Table VIII such that the k_{eff} at BOEC is 0.97.

Computed equilibrium cycle performance parameters are summarized in Table X. Compared to the performance of the preliminary design (displayed in

TABLE IX

Isotopic Compositions of the Assumed LWR-Discharge Feed Stream and the LBE Blanket (ATW) Heavy Metal Discharge

Isotope	25-yr-Cooled PWR TRU (wt%)	ATW-Discharge TRU (wt%)	ATW-Discharge TRU (wt%) After 1-yr-Cooling
^{234}U	0.000[a]	0.593	0.633
^{235}U	0.004[a]	0.152	0.152
^{236}U	0.002[a]	0.207	0.210
^{238}U	0.478[a]	1.292	1.292
^{237}Np	5.023	2.095	2.102
^{238}Pu	1.272	6.065	6.397
^{239}Pu	53.196	19.053	19.055
^{240}Pu	21.534	35.358	35.465
^{241}Pu	3.782	6.467	6.224
^{242}Pu	4.686	12.783	12.785
^{241}Am	8.967	5.267	5.504
^{242m}Am	0.014	0.485	0.483
^{243}Am	0.926	4.443	4.443
^{242}Cm	0.000	0.525	0.149
^{243}Cm	0.002	0.051	0.050
^{244}Cm	0.104	3.557	3.448
^{245}Cm	0.009	0.959	0.959
^{246}Cm	0.001	0.649	0.649

[a]It was assumed that 99.995% of the uranium is removed in the UREX process.

TABLE X

Performance Characteristics of the Proposed LBE-Cooled Blanket Point Design

TRU fraction in fuel (wt%)	
Inner zone	37.7
Middle zone	45.4
Outer zone	49.6
Multiplication factor	
BOEC	0.9702
EOEC	0.9174
Burnup reactivity loss (% Δk)	5.3
Core-average power density (kW/ℓ)	156.3
Power-peaking factor	
BOEC	1.46
EOEC	1.51
Peak linear power (kW/m)	
Inner zone	25.0 (at EOEC)
Middle zone	26.1 (at EOEC)
Outer zone	24.5 (at BOEC)
Discharge burnup (at.%)	
Average	26.7
Peak	40.4
Peak fast fluence (10^{23} n/cm^2)	
Inner zone	3.71
Middle zone	3.88
Outer zone	3.28
Net TRU consumption rate (kg/yr)	237
Equilibrium loading (kg/yr)	
LWR TRU	237
Recycled TRU	649
Total TRU	886
Heavy metal inventory (kg)	
BOEC	2661
EOEC	2542

Table III), the TRU inventory at BOEC is increased by 18% because of the increased number of assemblies, the extended buffer region, the modified enrichment zoning, and the use of a 25-yr–cooled LWR-discharge feed stream. Consequently, the average discharge burnup and the burnup reactivity loss are reduced slightly. An average discharge burnup of ~27% is achieved with a 3.5-yr fuel residence time; this discharge burnup would increase to ~28%, while staying within the peak fast fluence constraints, if the capacity factor were increased from the assumed 75% to 79%. The burnup reactivity loss for the point design is 5.3% with the assumed half-year cycle. If no other reactivity control measure is employed to compensate for this burnup reactivity loss and the transmuter is operated at a constant power by increasing the accelerator power, the required beam currents for a 1-GeV proton beam are 12.5 mA at BOEC and 35 mA at EOEC. The corresponding beam power at BOEC is similar to the value employed in the ATW roadmap, but the EOEC beam power is considerably larger. This range of beam power can be achieved practically since linear accelerators are believed to be capable of accelerating over 100 mA of protons to several giga-electron-volts.[6] However, to improve the overall system economics, it might be necessary to reduce the cycle length further or to employ other methods to compensate a part of this burnup reactivity loss. The highest TRU fraction in the charged fuel (i.e., the outermost zone enrichment) is ~50 wt%, which is well within the limit of the metallic dispersion fuel.

The adopted enrichment zoning results in similar power-peaking factors at BOEC (1.46) and EOEC (1.51). At BOEC, the peak linear power (24.5 kW/m) occurs in the outer fuel zone. Because of the increased spallation source intensity and nonuniform TRU depletion, the peak power location moves to the middle fuel zone (26.1 kW/m) at EOEC. (The peak of the batch-averaged power density at EOEC is highest in the inner blanket zone. However, because of the smaller number of batches used in the inner zone, the stage factor accounting for the higher power density of fresh fuel assemblies is smaller in the inner zone than in the middle zone. Consequently,

the peak linear power is higher in the middle zone than in the inner zone.) Note that the resulting peak linear powers in the three blanket zones are very close to each other as desired, and that they are well within the limiting value of 33 kW/m. The peak-fast-fluence value of 3.88×10^{23} n/cm^2 occurs in the middle blanket zone and is well within the assumed fast-fluence limit of 4.0×10^{23} n/cm^2.

The batch-averaged fission power produced by each fuel assembly and the fission power densities at the blanket axial midplane are shown for the proposed point design in Figs. 10 and 11, respectively. As shown in Figs. 10 and 11, the assemblies in the middle blanket zone generally produce more power than those in the inner and outer zones, and the assembly powers of the middle zone remain relatively constant over the irradiation cycle. The assembly powers in the inner zone increase ~15% on average over the irradiation cycle, while the assembly powers in the outer zone decrease by an average of ~5%. The highest assembly power of 5.1 MW occurs in one of the middle zone assemblies at EOEC. The coolant velocity required to remove this heat load is ~1.5 m/s for a coolant temperature rise of 150 K, which is well within the assumed velocity limit of 2.0 m/s.

V. CONCLUSIONS

The parametric studies leading to the proposed system point design have defined the characteristics of an LBE-cooled transmutation blanket that enables efficient consumption of LWR-discharge TRU. The key system objective of high ATW fuel discharge burnup (to minimize the number of successive recycle stages and associated TRU losses) was shown to be achievable in a configuration with comparatively high power density (enabling small system size and potentially favorable economics) and relatively low burnup reactivity loss (to reduce requirements for reactivity and/or source control). System design and operating characteristics that satisfy these goals while meeting key thermal-hydraulic and materials-related design constraints were preliminarily developed. Perhaps more significantly, a systematic approach was devised for meeting these key objectives

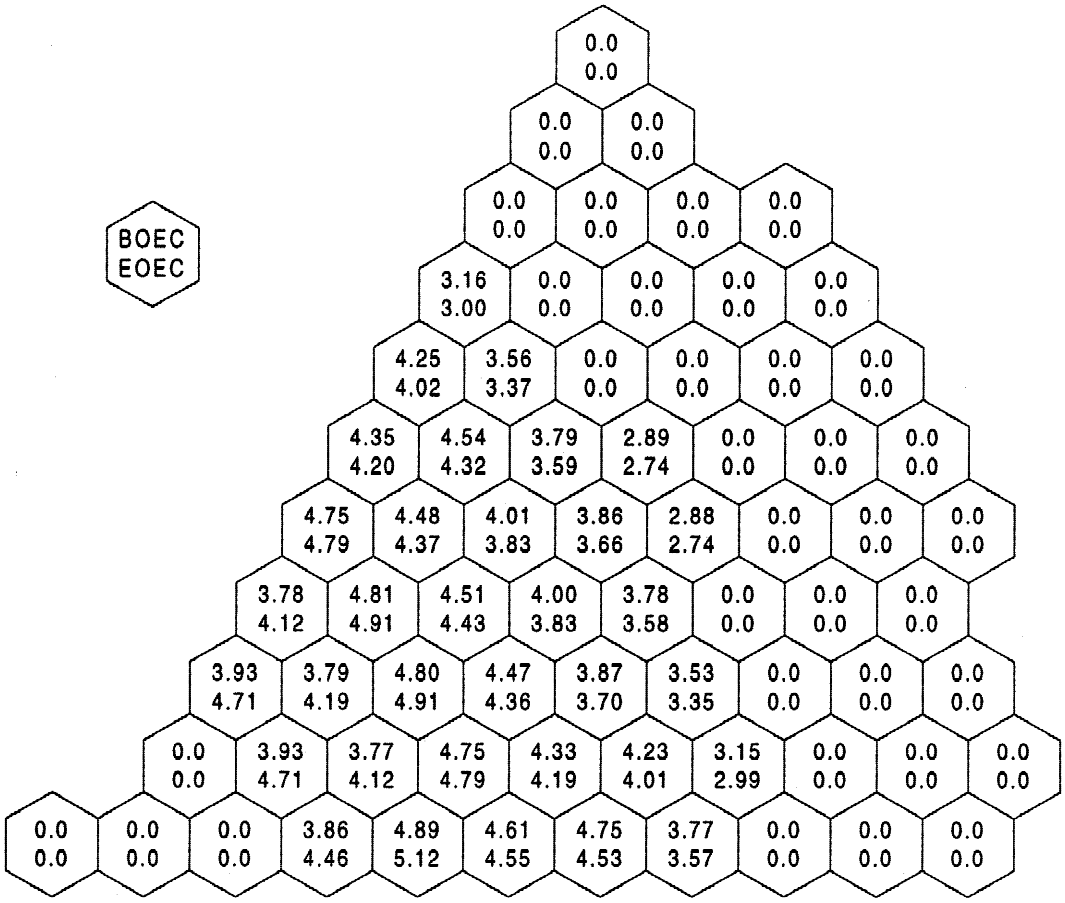

Fig. 10. Total assembly fission power for the LBE system point design (in megawatts).

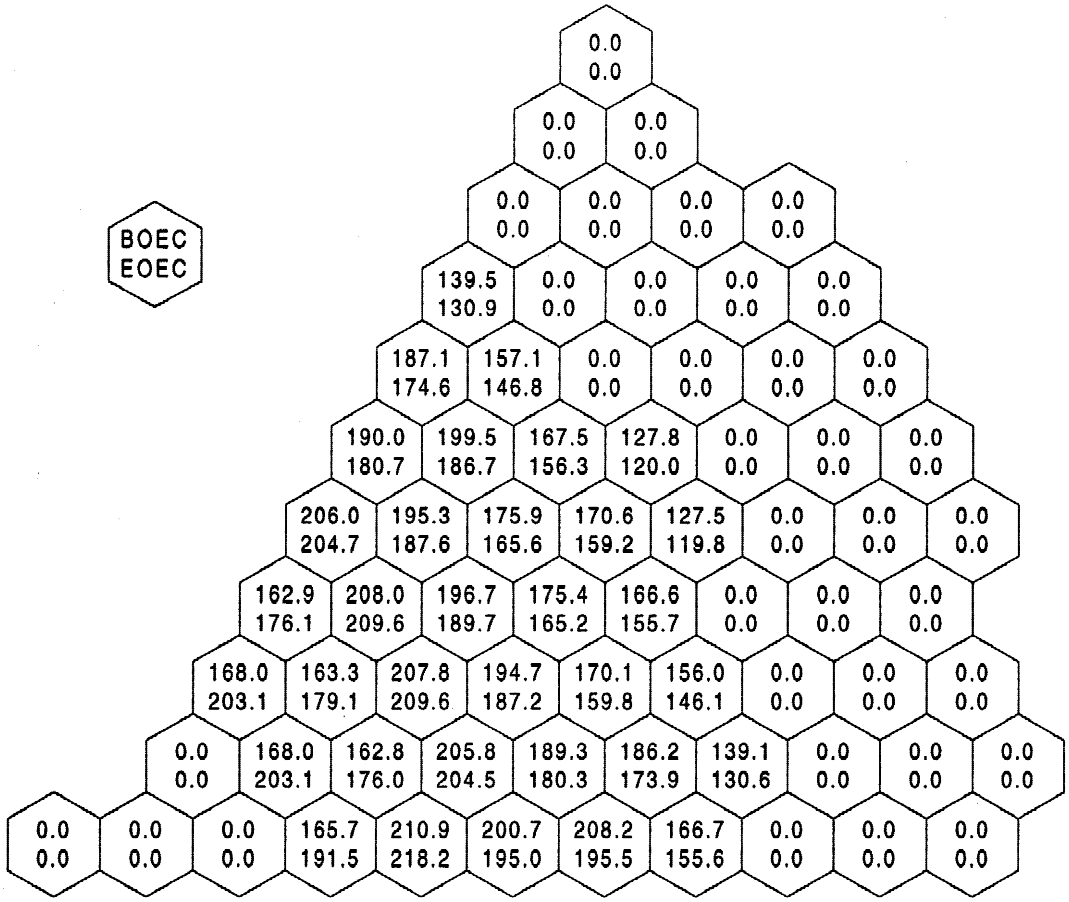

Fig. 11. Fission power densities at blanket midplane (in watts per cubic centimetre).

subject to the assumed constraints. This approach should greatly facilitate future efforts to optimize the system's performance, e.g., for updated values of the constraining variables or taking a broader set of performance objectives into consideration.

Two key assumptions made in developing the proposed point design are the power level of the transmutation system [840 MW(thermal)] and its minimum subcriticality level (k_{eff} = 0.97 at the start of cycle); both parameters strongly affect system characteristics and directly impact the accelerator beam power required per transmuter. The choice of transmuter (fission) power level is based largely on the recent design experience with the PRISM ALMR, which indicates that favorable economics and safety performance can be achieved with the 840-MW(thermal) system size. The applicability of this experience to the LBE-cooled ATW transmuter should be examined in future studies. With respect to degree of subcriticality, the assumed level is believed to be a good compromise between the competing objectives of minimizing accelerator power (favors high k_{eff}) and precluding the potential for criticality as a result of operational or accidental reactivity insertions (favors low k_{eff}). However, explicit dynamic and safety analyses will be required to optimize the choice of subcriticality level.

Future evaluations of system dynamic behavior and safety characteristics must be performed in conjunction with (a) development of the heat transport system (nuclear steam supply system), (b) design of the LBE spallation target and accelerator beam delivery system, and (c) development of the system control strategy. Key design objectives will be to incorporate passive safety features and to ensure that the thermal stresses resulting from planned and unplanned accelerator beam interruptions do not excessively limit the lifetime of transmuter structures and components. These system development efforts and supporting dynamic analyses are currently at an early stage.

With respect to transmutation performance, the current study has focused on the equilibrium-cycle mass flows, assuming that TRU losses during recycle are negligible. Future studies are needed to assess the impact of nonzero TRU losses on the fuel cycle mass flows in general (including fuel composition effects) and the waste streams in particular. Moreover, a blanket management/

control strategy should be developed for accommodating the evolution of fuel composition (and reactivity) during the transition to the equilibrium, as well as for variations in the LWR feedstock composition and other deviations from the equilibrium conditions.

Significant research and development (R&D) efforts will be required to confirm the feasibility of two key elements of the LBE system point design—adoption of LBE as target and coolant material and use of nonuranium fuels. These R&D requirements are discussed elsewhere.[3,11] Related system performance issues requiring attention include the activation of LBE coolant and the buildup of spallation products in the LBE target. These assessments should be conducted as part of a larger effort to characterize the waste generation for the entire ATW system—both during operation and in the stage of facility decontamination and decommissioning.

REFERENCES

1. "Accelerator-Driven Transmutation of Waste (ATW): A Six-Year Science-Based Technology Development Program," Rev. 0, Los Alamos National Laboratory (Mar. 2000).

2. D. J. HILL, G. VAN TUYLE, D. BELLER, B. BISHOP, T. COTTON, P. FINCK, B. HALSEY, J. HERCZEG, J. S. HERRING, D. LANCASTER, J. MARCH-LEUBA, H. LUDEWIG, T. SANDERS, B. SAVAGE, E. SCHWEITZER, C. SMITH, L. STEWART, M. TODOSOW, and C. WALTER, "A Roadmap for Developing ATW Technology: Systems Scenarios and Integration," ANL-99/16, Argonne National Laboratory (Sep. 1999).

3. F. VENNERI, D. CRAWFORD, H. KHALIL, N. LI, T. ALLEN, M. LOUTHAN, K. WOLOSHUN, A. BRUNSVOLD, C. EHRMAN, D. WADE, M. CAPPIELLO, M. CHADWICK, P. LISOWSKI, S. HAYES, J. HERCEG, and P. MAC DONALD, "Roadmap for the Development of Accelerator Transmutation of Waste: Target and Blanket System," LA-UR-99-3022, Los Alamos National Laboratory (Sep. 1999).

4. B. W. SPENCER, "The Rush to Heavy Liquid Metal Reactor Coolants—Gimmick or Reasoned," *Proc. 8th Int. Conf. Nuclear Engineering (ICONE 8)*, Baltimore, Maryland, April 2–6, 2000, ICONE-8729 (2000).

5. R. N. HILL, D. C. WADE, J. R. LIAW, and E. K. FUJITA, "Physics Studies of Weapons Plutonium Disposition in the Integral Fast Reactor Closed Fuel Cycle," *Nucl. Sci. Eng.*, **121**, 17 (1995).

6. "A Roadmap for Developing Accelerator Transmutation of Waste (ATW) Technology—A Report to Congress," DOE/RW-0519, U.S. Department of Energy (Oct. 1999).

7. E. L. GLUECKER, "U.S. Advanced Liquid Metal Reactor (ALMR)," *Prog. Nucl. Energy*, **31**, 43 (1997).

8. R. D. LEGETT and L. C. WALTERS, "Status of LMR Fuel Development in the United States," *J. Nucl. Mater.*, **204**, 23 (1993).

9. M. SALVATORES, I. SLESSAREV, A. TCHISTIAKOV, and G. RITTER, "The Potential of Accelerator-Driven Systems for Transmutation or Power Production Using Thorium or Uranium Fuel Cycles," *Nucl. Sci. Eng.*, **126**, 333 (1997).

10. P. A. FOMITCHENKO, "Physics of Lead-Cooled Reactors," *Proc. 1998 Frédéric Joliot Summer School in Reactor Physics*, Cadarache, France, August 17–26, 1998.

11. D. C. CRAWFORD, Argonne National Laboratory, Personal Communication (Aug. 2000).

12. B. J. TOPPEL, "A User's Guide to the REBUS-3 Fuel Cycle Analysis Capability," ANL-83-2, Argonne National Laboratory (1983).

13. W. S. YANG and H. S. KHALIL, "Analysis of the ATW Fuel Cycle Using the REBUS-3 Code System," *Trans. Am. Nucl. Soc.*, **81**, 277 (1999).

14. K. L. DERSTINE, "DIF3D: A Code to Solve One-, Two-, and Three-Dimensional Finite-Difference Diffusion Theory Problems," ANL-82-64, Argonne National Laboratory (1984).

15. R. D. LAWRENCE, "The DIF3D Nodal Neutronics Option for Two- and Three-Dimensional Diffusion Theory Calculations in Hexagonal Geometry," ANL-83-1, Argonne National Laboratory (1983).

16. G. PALMIOTTI, E. E. LEWIS, and C. B. CARRICO, "VARIANT: Variational Anisotropic Nodal Transport for Multidimensional Cartesian and Hexagonal Geometry Calculation," ANL-95/40, Argonne National Laboratory (1995).

17. H. HENRYSON II, B. J. TOPPEL, and C. G. STENBERG, "MC^2-2: A Code to Calculate Fast Neutron Spectra and Multigroup Cross Sections," ANL-8144, Argonne National Laboratory (1976).

18. W. M. STACEY, Jr., B. J., TOPPEL, H. HENRYSON II, B. A. ZOLOTAR, R. N. HWANG, and C. G. STENBERG, "A New Space-Dependent Fast-Neutron Multigroup Cross-Section Preparation Capability," *Trans. Am. Nucl. Soc.*, **15**, 292 (1972).

19. B. C. NA, P. WYDLER, and H. TAKANO, "OECD/NEA Comparison Calculations for an Accelerator-Driven Minor Actinide Burner: Analysis of Preliminary Results," presented at 2nd Workshop Utilization and Reliability of High Power Proton Accelerators, OECD Nuclear Energy Agency, Aix-en-Provence, France, November 22–24, 1999.

20. R. N. BLOMQUIST, "VIM—A Continuous Energy Monte Carlo Code at ANL," ORNL/RSIC-44, Oak Ridge National Laboratory (Apr. 1980).

21. M. J. BELL, "ORIGEN—The ORNL Isotope Generation and Depletion Code," ORNL-4628, Oak Ridge National Laboratory (1973).

22. R. N. HILL, Argonne National Laboratory, Personal Communication (June 2000).

Won Sik Yang (BS, nuclear engineering, Seoul National University, Korea, 1984; PhD, nuclear engineering, Purdue University, 1989) is an associate professor of nuclear engineering at Chosun University in South Korea. His background includes reactor physics, core design, and fuel cycle analysis.

Hussein Khalil (BS, nuclear engineering, Kansas State University, 1978; PhD, nuclear engineering, Massachusetts Institute of Technology, 1983; MBA, University of Chicago, 1996) is associate director of the Reactor Analysis and Engineering Division at Argonne National Laboratory. His background includes reactor physics, core design, and fuel cycle analysis.